# Diatomic Molecular Probes for Mid-IR Studies of Zeolites

**A. Zecchina**
*Dipartimento di Chimica Inorganica, Chimica Fisica e Chimica dei Materiali, Università di Torino, Via P. Giuria, 7, 10125 Torino, Italy*

**C. Otero Areán**
*Departamento de Química, Universidad de las Islas Baleares, 07071 Palma de Mallorca, Spain*

## 1 Introduction

Zeolites are tecto-aluminosilicates which can be described by the general formula $M^{n+}_{x/n}[(AlO_2)_x(SiO_2)_y]^{x-}\cdot zH_2O$, where M can be a metal cation or a proton. The Si/Al ratio in synthetic zeolites varies considerably; limiting extremes being 1:1 (lower ratio for zeolite X) to near infinity:1 (in silicalites). This provides a means to modulate the ionicity of the material, which increases with decreasing Si/Al ratio. The framework of every zeolite is constructed from tetrahedral building blocks, $TO_4$, where T is a tetrahedrally coordinated atom (*i.e.* Si, Al), as depicted in Scheme 1. An isolated $SiO_4$ group would carry a formal charge of $-4$, but in a solid having an O/T ratio of 2 (as found for all zeolites) the $SiO_4$ unit is neutral, because each oxygen atom is part of a bridge between two T atoms. However, the net formal charge of the $AlO_4$ units is $-1$, so that the zeolite framework is negatively charged.

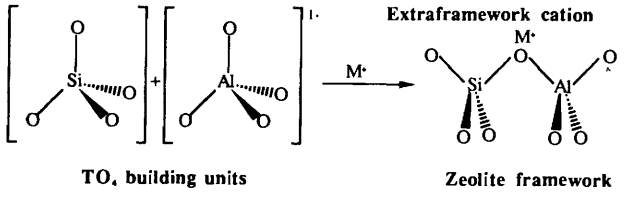


**Scheme 1**

The net negative charge is balanced by $M^{n+}$ cations, or by protons in the acidic form of the zeolite. These ions are not a part of the zeolite framework, and under the right conditions they can be exchanged by other cations. Such an exchange has little effect on crystal structure, which depends on the way in which the $TO_4$ units arrange themselves; it does affect, however, other relevant properties of the zeolite such as acidity and internal electric fields. Brønsted acidity arises from bridging Si(OH)Al groups in the protonic form of zeolites. Extraframework (charge-balancing) cations act at Lewis acid centres, in the broad sense, since they are electron acceptors. A different (and more important) source of Lewis acidity concerns structural defects and extraframework aggregates. Charge-balancing cations are also the main source of intrazeolite electric fields which have a strength of several V $nm^{-1}$, the actual value depending on cation charge and radius.

A characteristic feature of zeolites is their structural porosity. The framework of all zeolites defines regular systems of intracrystalline voids and channels of discrete size, usually in the nanometre range, accessible through apertures of well-defined molecular dimensions. This is a feature that differentiates zeolites from other microporous materials, like amorphous carbon or silica gel (which have irregular pore systems), and which places them in the same class as other molecular sieves. Zeolites containing rings consisting of 8, 10 and 12 oxygen atoms are denoted as small- medium- and large-pore materials. The corresponding pore openings are about 0.4, 0.55 and 0.73 nm in size, respectively. Recently, other zeotypes having extra-large pores have been synthesized: among them are cloverite (a gallophosphate molecular sieve), AlPO-8, VPI-5, and JDF-20, with present pore openings up to 1.2—1.4 nm in diameter.[1–3] Zeotypes are materials structurally related to zeolites, in which Si or Al atoms have been replaced by other atoms, *e.g.* Ga for Al or P for Si. For a detailed account see, *e.g.* ref. 4.

Their microporous framework structures, wide range of chemical composition and surface acidity, and the possibility of tuning internal electric fields by appropriate choice of extraframework cations, are key factors which render zeolites (and zeotypes) versatile materials for an increasing number of technological applications. Paramount among these is the use of zeolites as catalysts for the petrochemical industry, pollution control and the synthesis of speciality chemicals. They also serve as ion exchangers and molecular sieves. A more recent perspective is the proposed use of zeolites as host materials for host–guest composites. These are a kind of advanced materials where zeolites (or zeotypes) act as hosts for encapsulating and organizing molecules, crystalline nano-phases and supramolecular entities inside their pores. Space confinement and host–guest (electrostatic) interaction result in a type of composite materials with novel properties.[5,6] Potential applications are expected in a number of technological fields, such as photochemistry, optoelectronics, semiconducting devices and chemical sensors.

*Adriano Zecchina was educated at the University of Turin (Italy) where he is Ordinary Professor of Physical Chemistry. He has also spent a year at Bath University (UK) doing research on surface spectroscopy. Prof. Zecchina is a foreign member of the Faraday Division Council, and has acted as President of the Associazione Italiana di Chimica Fisica. His main research interests focus on the study of surface chemistry using spectroscopic techniques. He has co-authored over 150 scientific articles in that field, including three reviews.*

*Carlos Otero Areán was educated at the University of Madrid (Complutense) and obtained PhD degrees in chemistry from the universities of Bath (UK) and Madrid. He has carried out post-doctoral research at the French CNRS (Orléans) and at the University of Oxford (ICL). Currently, he is Professor of Inorganic Chemistry at the Universidad de las Islas Baleares (Spain), where his main research interests are in several aspects of solid state and surface chemistry.*

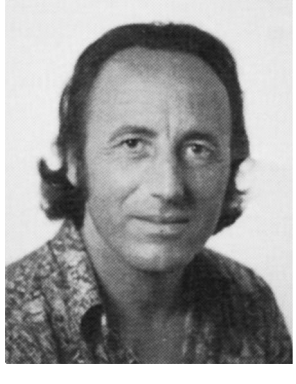

Zeolite and zeotype cavities can be considered as nanoreactors where adsorbed molecules are guided to react following specific paths dictated by (*i*) the electrostatic forces acting inside the cavities, (*ii*) the distribution of sites on the internal surface, (*iii*) the spatial restrictions imposed by the dimension and shape of the void space, and (*iv*) limitations on diffusion paths imposed by the regular organization of (intersecting) channels All of these points can be summed up under the synthesizing concept of host–guest interactions, so fruitfully used to understand many properties of supramolecular and enzyme–substrate systems More specifically, electrostatic fields operating inside cavities and channels can lead to the formation of internal adducts characterized by a profound deformation of the electron distribution of perturbed molecules with simultaneous polarization, and appearance of new nucleophilic and electrophilic regions and ultimately of new chemical properties In the case of proton-exchanged zeolites the internal adducts can be more properly classified as hydrogen-bonded complexes, which under suitable conditions can evolve towards protonated species and initiate the chain of Brønsted acid-catalysed reactions that (together with shape selectivity) make acidic zeolites so important in petrochemistry

Precise characterization of the solid is a prime requirement for understanding intra-zeolite processes, and it should also assist in designed synthesis of new materials To this end, crystallographic methods are efficiently complemented with spectroscopic techniques, mainly IR and MAS NMR spectroscopy, which have the potential to furnish information about the nature of surfaces and of adsorbed species Mid-IR spectroscopy (4000—400 $cm^{-1}$) using appropriate probe molecules is a powerful technique for studying the internal surface of zeolites The method is indirect, in the sense that it depends on a suitable choice of spectroscopic probes which render the zeolite cavities IR-readable Probe molecules most often used are CO, $N_2$ and $H_2$, although many others have been utilized The observables are the changes in vibrational frequency and intensity, and the induced vibrational modes of the probe molecule as a result of interaction with the zeolite (internal) surface Induced changes of skeletal and O—H vibrations can also be highly informative A related aspect is the use of vibrational spectroscopy to follow chemical processes taking place in the intra zeolite space (reaction dynamics) Time-resolved (sub-second) FTIR spectroscopy has the potential to detect intermediate species in a reaction chain, for example, in a study of the interaction of acetylenes with an H-ZSM 5 zeolite,[7] prior formation of an H-bonded complex and subsequent transformation into a protonated species, followed by polymerization, could be analysed This subject, however, is beyond the scope of the present review We shall focus on the use of diatomic probe molecules for mid-IR studies of (*i*) OH groups and Brønsted acidity, (*ii*) internal electric fields, and (*iii*) extraframework species Cation location can also (in some instances) be discerned by both mid- and far-IR spectroscopy, the latter subject was recently reviewed by Baker *et al*.,[8] while Ward[9] has given a detailed account of early work on mid-IR characterization of zeolites

## 2 General Background

### 2.1 Molecular Probes

The information which can be obtained from IR spectra using molecular probes concerns

(*i*) Surface hydroxy groups, both silanols and bridged Si(OH)Al groups, which are the source of Brønsted acidity Ideally, acid strength should also be quantified

(*ii*) Lewis acidity, which depends mainly on framework structural defects and on extraframework species The latter are very small metal oxide particles generated during thermal treatment of the zeolite

(*iii*) Other types of structural defects, such as hydroxy nests or occluded material

(*iv*) The nature and location of extraframework cations

(*v*) Internal electric fields

Changes undergone by the molecular probe can also be informative of the nature of chemical processes expected to take place within the intra-zeolite space This aspect, however, cannot strictly be considered as a part of zeolite characterization

Ideally, molecular probes for IR studies should satisfy the following requirements (*i*) small size, so that the probe has unimpeded access to channels and cavities, (*ii*) detectable spectroscopic response triggered by interaction with the zeolite surface, this response should discriminate between surface sites of different nature and should allow quantitative determinations to be performed, (*iii*) extinction coefficients for characteristic vibrational modes should be high, so as to lead to *optimum* detection sensitivity, (*iv*) the probe molecule should be responsive not only to the surface site but also to its close environment, this is particularly relevant for detecting bifunctional surface sites, and (*v*) in order to avoid alterations of the material under test, probe–surface interaction should be weak, the foregoing considerations on spectroscopic response notwithstanding

Many molecular probes have been used to characterize different aspects of zeolite surfaces, among them $H_2$, $N_2$, CO, $N_2O$, pyridine and several hydrocarbons None of them, however, satisfies entirely all of the above requirements Concurrent use of two (or more) different probes can help to resolve specific problems CO, $N_2$ and $H_2$ have kinetic diameters of 0 376, 0 364 and 0 289 nm, respectively, so that they all satisfy the size requirement for acting as probe molecules in most zeolites Interaction modes and consequent spectroscopic response will now be briefly outlined

Carbon monoxide has a small dipole moment ($\mu$ = 0 112 D) which varies during vibration, thus rendering the C—O stretching mode IR-active For the free molecule the fundamental $\bar{\nu}$(C—O) value is 2143 $cm^{-1}$, which is expected to change little on physical adsorption Interaction with an ionic surface is expected to produce a more significant negative shift of the CO stretching frequency for adsorption *via* carbon at an anion site or *via* oxygen at a cation site Large positive shifts result from adsorption *via* oxygen to an anion site or *via* carbon at a cation site [10] The reason for the reversed sign of the frequency shift is that the dipole moment derivative, $d\mu/dr$, changes sign when the orientation of the dipole axis with respect to the external electric field is reversed Extensive experimental evidence proves that CO interacts *via* the carbon end with cations in ionic metal oxides and halides, leading to hypsochromic shifts in the 10—70 $cm^{-1}$ range, the actual value depending on cation size and charge For $d^0$ cations having a net charge $\leqslant 2+$, interaction with CO is dominated by electrostatic effects ion–dipole (and quadrupole) interactions and CO polarization, and the frequency shift of the C—O stretching mode arises mainly from the vibrational Stark effect and from a 'wall effect' stemming from increased Pauli repulsion when the CO molecule vibrates against the solid surface [11] When cations having a net charge larger than 2+ or transition metal ions are involved, chemical effects due to $\sigma$ donation (from the CO $5\sigma$ orbital) and $d$–$\pi$ back donation can lead to a more complex situation It should also be noted that inside zeolite cavities multiple interactions can develop, which must be carefully analysed

Both dinitrogen and dihydrogen, being homopolar molecules, are IR-inactive when unperturbed However, in presence of an electric field, **E**, an induced dipole moment, $\alpha$**E** (where $\alpha$ is the polarizability) develops which varies during vibration, thus rendering the fundamental transition IR-active For dinitrogen, *ab initio* calculations[12,13] (both in the SCF approximation and with electron correlation) of the interaction with alkali metal cations showed that the *optimum* configuration corresponds to the linear arrangement $M^+ \cdots N{\equiv}N$ (where $M^+$ stands for the metal ion) This interaction leads to a decreased N—N bond length and to a positive shift of the $\bar{\nu}$(N—N) stretching frequency with respect to the (Raman active) gas-phase value of 2331 $cm^{-1}$ The intensity of the field-induced IR absorption is proportional to the second power of the electric field,[14] or more exactly to the square of the field component directed along the molecular axis

*Ab initio* calculations[13,15] for the interaction between dihydrogen and alkali metal cations led to the geometry **1** depicted in Scheme 2, which results in lengthening of the H—H bond and a negative frequency shift from the position of the Q branch vibration of free $H_2$ However, when cation–anion (Lewis acid–base) pairs were considered,[16,17] dihydrogen was found to interact simultaneously with

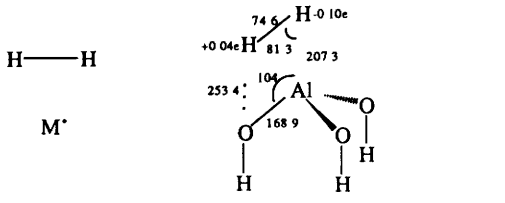


1 2 (bond lengths in pm)

Scheme 2

both ions This is shown in Scheme 2 (**2**) for an adsorption site modelled by the $Al(OH)_3$ cluster with standard bond angles and bond lengths In species **2** adsorbed dihydrogen becomes slightly polarized, which renders it IR-active with an H−H stretching frequency lowered with respect to the gas-phase value of 4163 $cm^{-1}$ An important feature is that the adsorbed molecule acts as a probe for the surface acid–base pairs, rather than only for the cation site

### 2.2 Procedures

Mid-IR studies of zeolites are usually performed in the transmission mode, since transparency is generally good However, in the high-frequency range scattering can sometimes be a serious problem, particularly when dealing with materials which have been synthesized as relatively large crystallites Diffuse reflectance measurements can help to overcome this problem

Studies concerning probe molecules make use of zeolite self-supporting wafers of 3—6 mg $cm^{-2}$, made by compacting the powdered material at a pressure of about 5000 kg $cm^{-2}$ The lowest possible pressure should be used, so that the crystal structure is not distorted Use of self-supporting wafers facilitates thermal activation of the zeolite sample prior to dosing with the appropriate gas (probe) Activation aims at removal of adsorbed water (and other atmospheric contaminants) and is usually performed by heating the zeolite wafer in a dynamic vacuum for several hours at a temperature of about 650 K Higher temperatures are likely to cause severe alteration of the zeolite, particularly dealumination, with attendant formation of extraframework species and lattice defects IR cells are currently in use which facilitate *in situ* thermal activation, dosing with the probe gas and recording the IR spectrum at low temperature, usually at a nominal value of 77 K sample wafer cooled with liquid nitrogen This last requirement is mandatory when dealing with spectroscopic probe molecules which show only a very weak interaction with the zeolite, among them $H_2$ and $N_2$

## 3 Structural Hydroxy Groups in Proton-exchanged Zeolites: Silanols and Brønsted Acid Sites

Two main types of OH groups are present in the protonic form of zeolites silanols (**3**) and bridging hydroxy groups (**4**), they are depicted in Scheme 3 It should be noted that in species **4** Si−O and Al−O bond lengths are different $d(Si-O) < d(Al-O)$

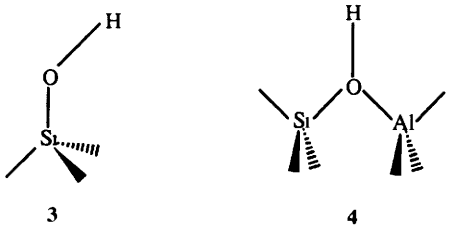


3 4

Scheme 3

Silanols are mainly found at external surfaces, where they saturate silicon dangling bonds associated with framework truncation Nevertheless, silanols also occur at internal lattice defects, arising mainly from partial dealumination In this case a local cluster of silanols is formed, which has been termed a silanol nest Isolated silanols on external surfaces are characterized by a sharp IR absorption band in the 3750—3745 $cm^{-1}$ range When silanols occur at internal sites, weak electrostatic perturbations cause a downward shift (and broadening) of the IR stretching band, which then appears at 3720—3700 $cm^{-1}$ Stronger, hydrogen-bonded interactions (*e g* in hydroxy nests) result in very broad IR absorption bands in the 3650—3200 $cm^{-1}$ range [18]

Bridging OH groups, which are the active sites in acidic catalysis, are found in two different wavenumber ranges 3650—3600 and 3580—3530 $cm^{-1}$ The high-frequency range corresponds to OH groups vibrating in large cavities, formed by greater than eight-membered rings, while in smaller voids the low-frequency range is observed This can be typified by the faujasite-type zeolites (FAU) which show O−H bands around 3650 and 3550 $cm^{-1}$, the actual value depending on Si/Al ratio The FAU-type structure is depicted in Fig 1, there are four different oxygen atoms, O(1)—O(4) Neutron diffraction studies[19] have shown that preferred proton sites are near O(1) and O(3) The proton at site 1 points into the supercage, while that at site 3 is directed into the sodalite unit where it interacts with nearby oxygen atoms Such an electrostatic interaction (related to the inverse of the square of the H−O distance) causes a bathochromic shift with respect to the unperturbed OH group at site 1 This explains the two IR absorption bands 3650 $cm^{-1}$ for OH groups at site 1 and 3550 for those at site 3 In agreement with this assignment, the high-frequency band is strongly perturbed (downward shifted) by adsorbed $N_2$ or CO, while the 3550 $cm^{-1}$ band remains unaffected, because the sodalite cage is not accessible to these gases It should also be noted that the O−H stretching wavenumber cannot be directly correlated with acid strength

When considering only wavenumbers corresponding to vibrations of OH groups in cages (or channels) with dimensions exceeding those of an eight-membered ring, a linear correlation was found between $\bar{\nu}$(O−H) and the average (Sanderson) electronegativity of the zeolite framework With increasing Sanderson electronegativity, $S$, which corresponds to increasing Si/Al ratio, OH groups vibrating in large cavities shift to lower wavenumbers following the equation $\bar{\nu}(O-H) = 4274 - 158\,576S$, as determined by Jacobs and Mortier [20] Since this empirical relation holds for a large number of zeolites, irrespective of structure type, it is inferred that small differences in Si(OH)Al bond angles have little influence on the O−H stretching frequency Because of the electrostatic effects already mentioned, hydroxy groups in eight-membered (or smaller) rings do not follow the above equation

A different example is furnished by mordenite (MOR) This is a zeolite wich has a pseudo-unidimensional pore system (the main channels) with an elliptical cross section, 0 65 × 0 70 nm in diameter, defined by twelve-membered rings of $TO_4$ tetrahedra The channel wall has side pockets circumscribed by eight-membered rings which are accessible through windows with a free diameter of 0 39 nm Accessible cation (or proton) sites are located on the walls of the main channels (sites B and C) and on the side pockets (site A), as depicted in Fig 2

A detail of the bridging OH spectrum is shown in Fig 3 The corresponding IR absorption band has a maximum at 3609 $cm^{-1}$, and is highly asymmetric on the low-frequency side Computer deconvolution showed two components centred at 3612 and 3585 $cm^{-1}$, respectively They were assigned[21] to acidic hydroxy groups vibrating in the main channels (high-frequency component) and in the side pockets (low-frequency component) Note the larger half-width of the low-frequency component, which results from electrostatic perturbation of OH groups within side pockets

Relevant parts of the FTIR spectra[21a 22] of CO and $N_2$ adsorbed at liquid nitrogen temperature on H MOR are shown in Fig 4 Only the main points will be discussed here, details are contained in the original references In the O−H stretching region, IR absorption bands are observed at 3747 (silanols) and at 3609 $cm^{-1}$ (bridging OH groups), they are both affected by CO and $N_2$ adsorption The silanol band is partially eroded by interaction with the probe molecules, at the highest doses shown in the spectra Dinitrogen shifts the 3747 $cm^{-1}$ band down to 3710 $cm^{-1}$ ($\Delta\bar{\nu} = -37$ $cm^{-1}$), while for carbon monoxide the corresponding shift amounts to

(*a*)

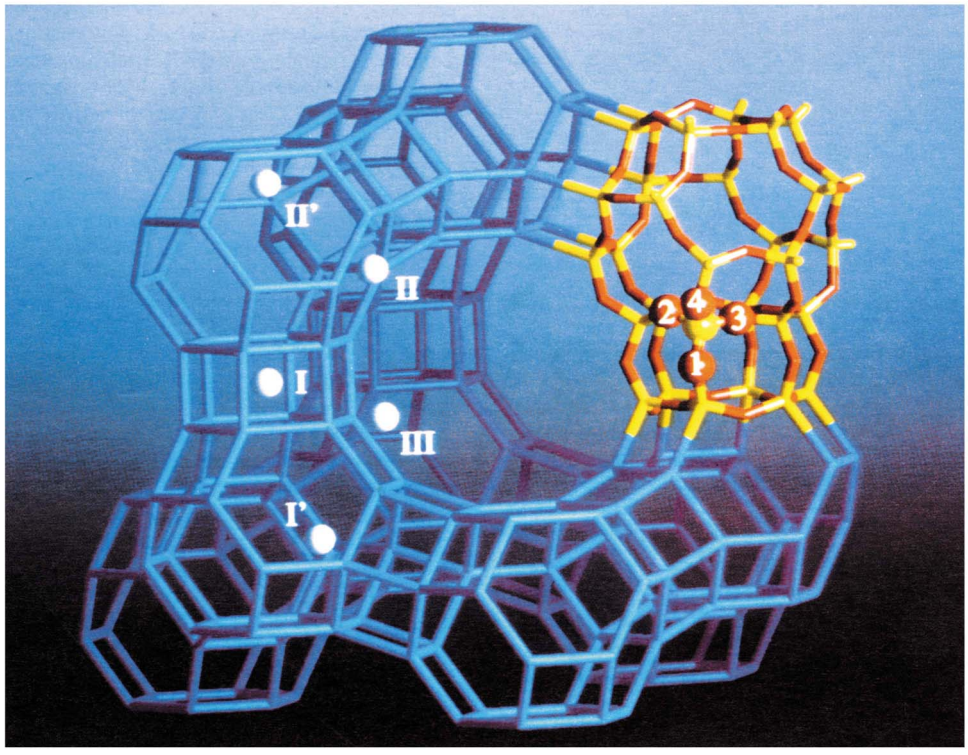


(*b*)

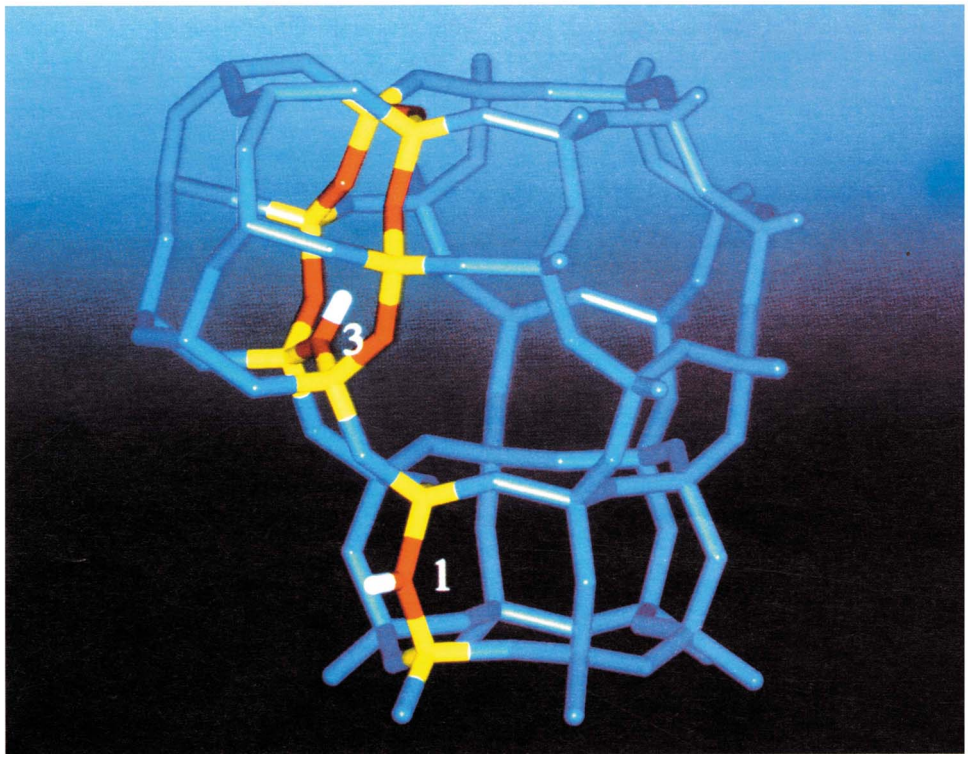


**Figure 1** (*a*) The faujasite type structure showing the 12 ring leading to the supercage, and the 6 rings which define apertures into the smaller sodalite cage Extraframework cation sites (I—III) are depicted, as well as the four different (1—4) anion sites (*b*) Detail showing the orientation of the bridging OH groups at sites O(1) and O(3)

−87 cm $^{-1}$ Qualitatively, this was the expected behaviour, since CO is a stronger Lewis base The IR absorption band corresponding to acidic OH groups (centred at 3609 cm $^{-1}$) is more strongly affected by the adsorbed gases A downward shift of −109 cm $^{-1}$ is observed for interaction with $N_2$, while for CO this shift is −294 cm$^{-1}$ Corresponding half-widths are 60 cm $^{-1}$ for $N_2$ and 175 cm$^{-1}$ for CO, which should be compared with the half-width value of 40 cm $^{-1}$ for the unperturbed O−H stretching band at 3609 cm $^{-1}$ Downward shifts, increased band width and increased intensity are precisely the effects predicted by the classical theory of hydrogen

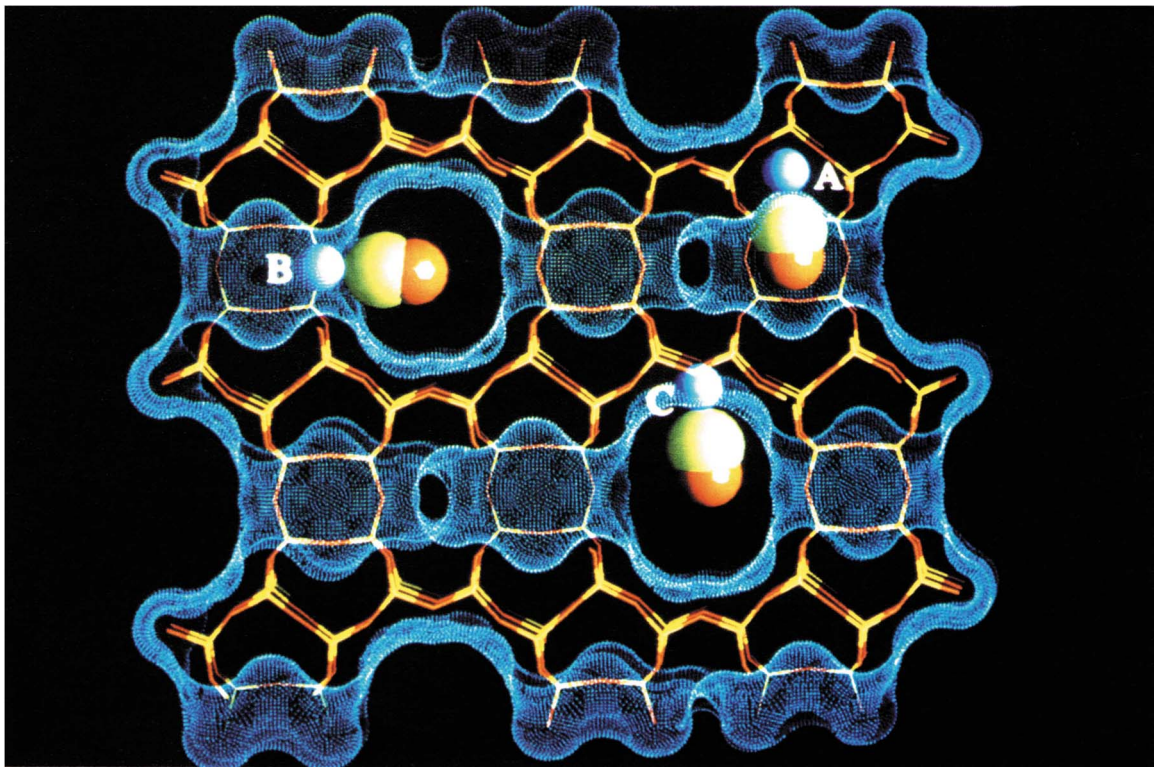


**Figure 2** The mordenite structure (viewed along the main channels) showing cation sites and adsorbed CO molecules. Dots outline Connolly surfaces obtained using a probe molecule having a radius of 0.14 nm. (Further details can be found in ref. 7).

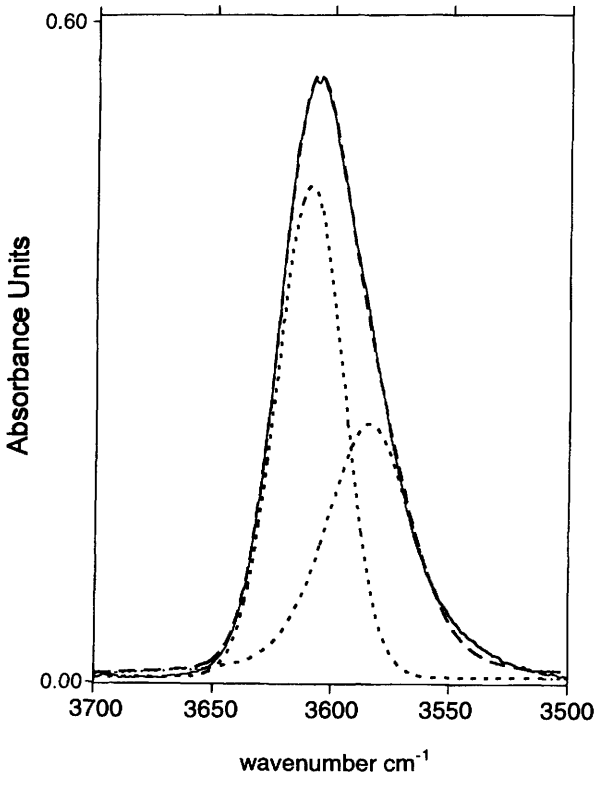


**Figure 3** Computer deconvolution of the 3609 $cm^{-1}$ O–H stretching band in H-MOR: components at 3612 and 3585 $cm^{-1}$. The solid line is the experimentally observed spectrum.
Reprinted with permission from ref. 21(*a*).

bonding, and the three magnitudes are directly correlated. The observed frequency changes upon interaction of the zeolite OH groups with the probe molecules are summarized in Scheme 4. A further detail which deserves comment is that progressive erosion of the 3609 $cm^{-1}$ band by both CO and $N_2$ is not uniform. The high-frequency component (3612 $cm^{-1}$, Fig. 3) is consumed faster than the low-frequency counterpart. This is in agreement with the expected higher difficulty for the probe molecules to gain access to the side pockets, while OH groups in the zeolite main channels are readily available.

The bathochromic shift, $\Delta\bar{\nu}$(OH), of the OH stretching band upon interaction with probe molecules is often used as a quantitative measurement of Brønsted acidity.[23] For carbon monoxide, an empirical relationship was established by Paukshtis and Yurchenko[24] between proton affinity, *PA*, and the value of $\Delta\bar{\nu}$(OH) referred to the corresponding value for isolated silanols having adsorbed CO, $\Delta\bar{\nu}$(SiOH). This relationship is as in eqn. (1).

$$PA/\text{kJ mol}^{-1} = 1390 - 442.5\log|\Delta\bar{\nu}(\text{OH})/\Delta\bar{\nu}(\text{SiOH})| \quad (1)$$

The lower the *PA* value, the higher is the Brønsted acidity of the OH group. This equation, however, should be used with caution when analysing the catalytic activity of zeolites in processes involving protonation of a reactant molecule. Proton transfer leads to charged species which interact with the (charged) zeolite framework, and the energy balance of the process can thus be significantly affected. For analogous reasons, the above relationship between *PA* and $\Delta\bar{\nu}$(OH) can lead to dubious results when it is used to compare intrazeolite processes with those occurring in the gas phase or in solution. It should also be noted that Brønsted acidity can be strictly defined only in terms of the reactant molecule, which acts as a proton acceptor.

Besides frequency shifts, the intensity of the perturbed OH band, or its half-width, can also be used to quantify interaction with probe molecules. However, since the intensity increase is directly correlated with the frequency shift, the shifted components of a complex OH band have different specific absorbance. Hence, determination of the relative amounts of the various hydroxy groups present in the sample becomes possible[23d,25] only when extinction coefficients can be evaluated.

Fig. 4 also shows the C–O and N–N stretching regions of H-MOR with increasing amouts of the adsorbed molecular probes. For CO, three IR absorption bands are observed, at 2138, 2172 and

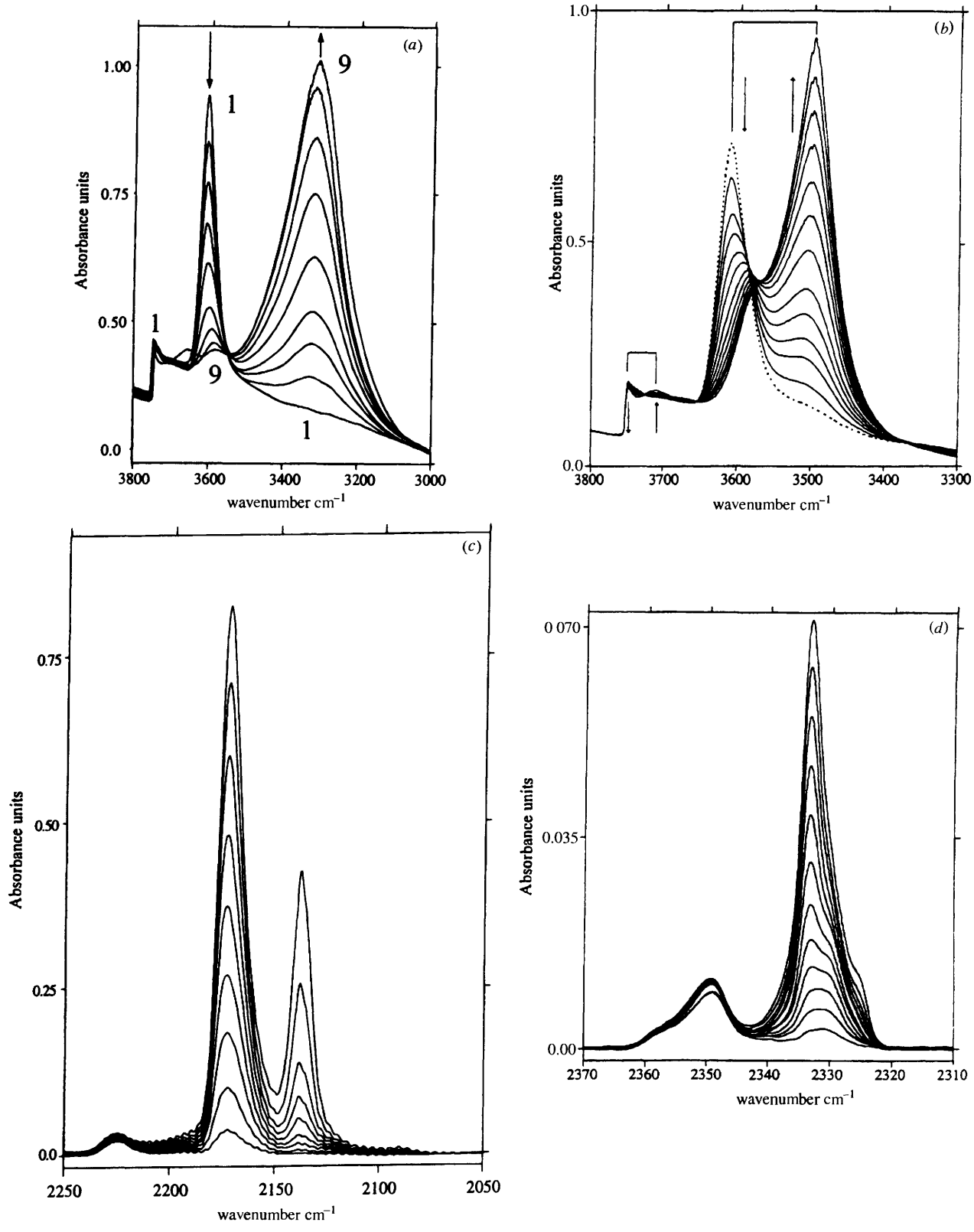


**Figure 4** (*a*) O–H stretching region of H-MOR outgassed at 673 K (spectrum 1) and the effect of increasing doses of adsorbed CO (spectra 2–9): equilibrium pressure from $10^{-2}$ to 20 Torr (1 Torr = 133.3 Pa). (*b*) Effect of adsorbed $N_2$, other details as above. (*c*) C–O stretching region. (*d*) N–N stretching region. All spectra were taken at liquid-nitrogen temperature. Those in parts (*c*) and (*d*) were background-subtracted. Reprinted with permission from ref. 21(*a*) [parts (*a*) and (*c*)] and ref. 22 [parts (*b*) and (*d*)].

2225 $cm^{-1}$ [Fig. 4(*c*)]. The 2138 $cm^{-1}$ band, which only becomes prominent for comparatively high CO equilibrium pressures, was assigned[21a] to physisorbed (liquid-like) CO inside the zeolite channels. Note its complex structure, which arises from hindered rotation.[21a,26] The 2225 $cm^{-1}$ band monitors extraframework species (Lewis acid sites), which will be considered in Section 5. The 2172 $cm^{-1}$ band corresponds to the C–O stretching of carbon monoxide interacting (*via* the carbon end) with the proton in bridging Si(OH)Al groups. Note that, although the band is asymmetric in the low-frequency side, the perturbation of the C–O stretching

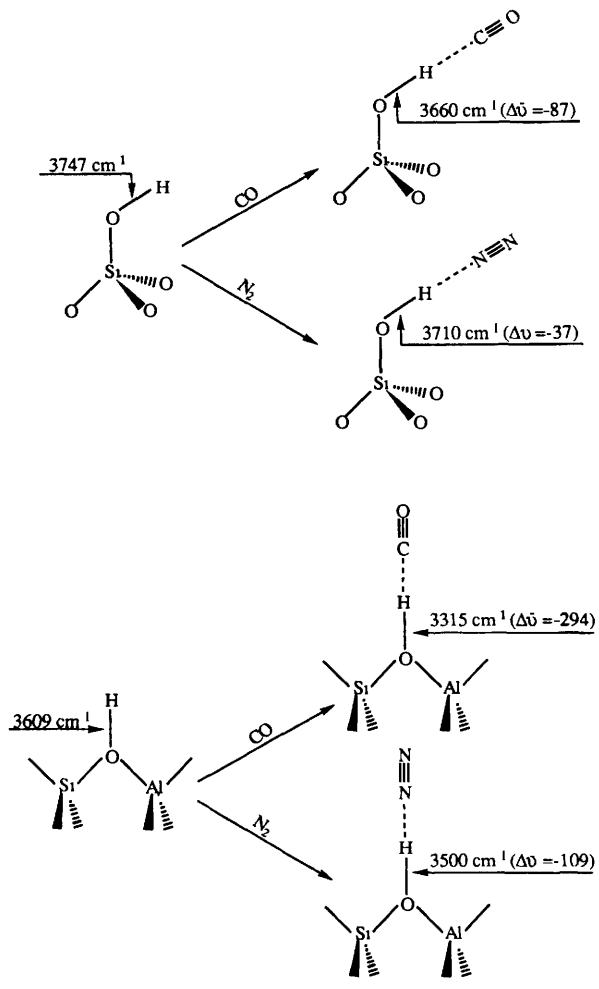


**Scheme 4**

vibration is not sensitive enough to discriminate between the two types of bridging OH groups main channels and side-pockets For $N_2$, the (complex) band corresponding to extraframework species is now found in the 2345—2360 cm $^{-1}$ range OH ··· $N_2$ species give a complex N—N stretching spectrum with components at 2325, 2330 and 2333 cm$^{-1}$, they correspond, respectively, to $N_2$ molecules interacting with silanols, and with OH groups in side-pockets (2330 cm$^{-1}$) and in the main channels (2333 cm $^{-1}$) The observed frequency range spans the (Raman active) gas-phase value of 2331 cm$^{-1}$ (Section 2 1) However, the Raman spectrum (taken in our laboratory) of dinitrogen adsorbed, at 240 K, on silicalite (a purely siliceous zeolite) gave a $\bar{\nu}$(N—N) value of 2321(± 2) cm $^{-1}$ Taking this as the reference value, all the observed N—N stretching maxima [Figure 4(*d*)] are upward shifted, as expected Note that $N_2$ is a more sensitive probe than CO for monitoring OH groups Two main factors contribute to this improved performance (*i*) absence of a contribution from liquid-like species (because unperturbed $N_2$ is IR-inactive), and (*ii*) weaker interaction with hydroxy groups,which results in enhanced selectivity

## 4 Charge-balancing Cations and Electric Fields

Adsorbed probe molecules can be used for IR monitoring of charge-balancing cations and their associated electric fields Alkali-exchanged ZSM-5 zeolites provide a good example ZSM-5, structure type MFI in IUPAC nomenclature, is a silicon rich zeolite which has a three dimensional pore system consisting of two intersecting sets of tubular channels (*ca* 0 55 nm in diameter) defined by ten-membered rings of $TO_4$ tetrahedra, as shown in Fig 5 IR spectra of CO adsorbed, at liquid nitrogen temperature, on $M^+$ ZSM 5 (M = Na, K, Rb, Cs) are depicted in Fig 6 They all show a main IR absorption band which, for low CO doses, was found to peak at 2178, 2166, 2162 and 2157 cm $^{-1}$ for $Na^+$ to $Cs^+$, respectively This cation-specific band has been assigned[27] to the fundamental C—O stretching of carbon monoxide perturbed by the corresponding metal ion [Fig 5(*b*)] Observed wavenumbers are all higher than the 2143 cm $^{-1}$ value for free CO, as expected for an $M^+$ ··· CO interaction (Section 2 1) A linear dependence was found between the C—O stretching frequency and the parameter $1/(R_M + R_{CO})^2$, where $R_M$ is the cation radius and $R_{CO}$ = 0 21 nm By using calculated values of $\bar{\nu}$(CO) for the molecule in the presence of an axial electric field,[11] the field strength due to charge balancing cations (and surrounding anions) has been experimentally determined from the corresponding IR frequencies [27a] The values obtained vary from 6 3 V nm$^{-1}$ for Na-ZSM 5 down to 2 4 V nm $^{-1}$ for Cs-ZSM-5 Slightly smaller values were observed for alkali-exchanged mordenites [21a] The whole set of results is summarized in Fig 7 Although the actual values reported here must be regarded as being only a first approximation, mainly because of simplifications made in the direct use of the $\bar{\nu}$(CO) *vs* electric field relationship,[11 27b] it should be clear that IR molecular probes constitute a valuable means for experimental determination of intrazeolite electric fields

A similar approach was taken by Cohen de Lara *et al* [14 28a] and by Bose and Forster[28b] who determined the electric field in zeolites Na-A, NaCa-A and Ca-A from the integrated IR intensities of adsorbed dinitrogen and carbon monoxide Values in the 5–8 V nm $^{-1}$ range were obtained, which are consistent with results from a theoretical calculation of the electrostatic field assuming an ionic model for the zeolite [28] Although more refined values are desirable, the order of magnitude of intrazeolite electric fields seems to be well established, and also their dependence on charge-balancing cation and zeolite structure

For $d^n$ cations more complex situations can arise as a result of chemical interactions involving the cation *d* orbitals (or hybrids) and $\sigma/\pi$ orbitals of the probe molecule Thus, when $Cu^+$-ZSM-5 was probed with CO, an adduct stable at room temperature was found[29a] which showed a CO IR absorption band at 2157 cm $^{-1}$, this is significantly lower than the corresponding value of 2178 cm $^{-1}$ for CO/Na-ZSM-5 Since the cation radii are in the order $r(Cu^+) < r(Na^+)$, it is clear that electrostatic interactions alone would not explain the observed spectroscopic results Dinitrogen was also found[29b,c] to form adducts with $Cu^+$ ions in $Cu^+$-ZSM-5 and $Cu^+$-MOR These adducts, which are stable at 298 K, showed an N—N stretching frequency of 2295—2299 cm $^{-1}$, *i e* downward shifted with respect to free $N_2$ The whole set of results can be rationalized in terms of chemical interaction involving molecular orbitals (MO) of the probe molecule and suitable d, s, p orbitals of the metal cation For CO, $\sigma$-donation through the weakly antibonding $5\sigma$ MO raises $\bar{\nu}$(CO), while back-donation to the antibonding $2\pi$ MO lowers it The net effect is a small hypsochromic shift, as compared to free CO For dinitrogen, the corresponding MOs are $3\sigma_g$ which acts as an electron donor, and the empty $1\pi_g$ which is the electron acceptor [30] In this case both the $\sigma$-donor and the $\pi$-acceptor interactions weaken the N≡N bond, thus explaining the observed bathochromic shift in the $Cu^+$ ··· $N_2$ adduct

Appropriate IR probe molecules can be used to test not only charge balancing cations, but also their local environment This was shown in a comparative study[17] of $H_2$ and CO adsorption for a series of zeolites having increasing ionicity, *i e* decreasing Si/Al ratio Na ZSM-5, Na MOR, Na-Y, Na-X, and the sodium form of Linde 4A Diffuse reflectance IR spectra of dihydrogen adsorbed at liquid nitrogen temperature on these zeolites are shown in Fig 8, a complete assignment of these spectra can be found in the original article Briefly, Na-ZSM 5 presents only a single IR absorption band (at 4110 cm $^{-1}$) consistent with a single type of cation site For Na MOR two absorption maxima are observed 4108 and 4125 cm $^{-1}$, as expected for two different cation sites (Section 3) The faujasite-type zeolites, X and Y, also show complex spectra, which were explained[17 31] in terms of the different cation sites (Fig 1) and their relative population Finally, two IR absorption maxima are observed for Na-A Structural data for this zeolite locate cations mainly near the centre of the six membered rings forming the sodalite cages

(*a*)

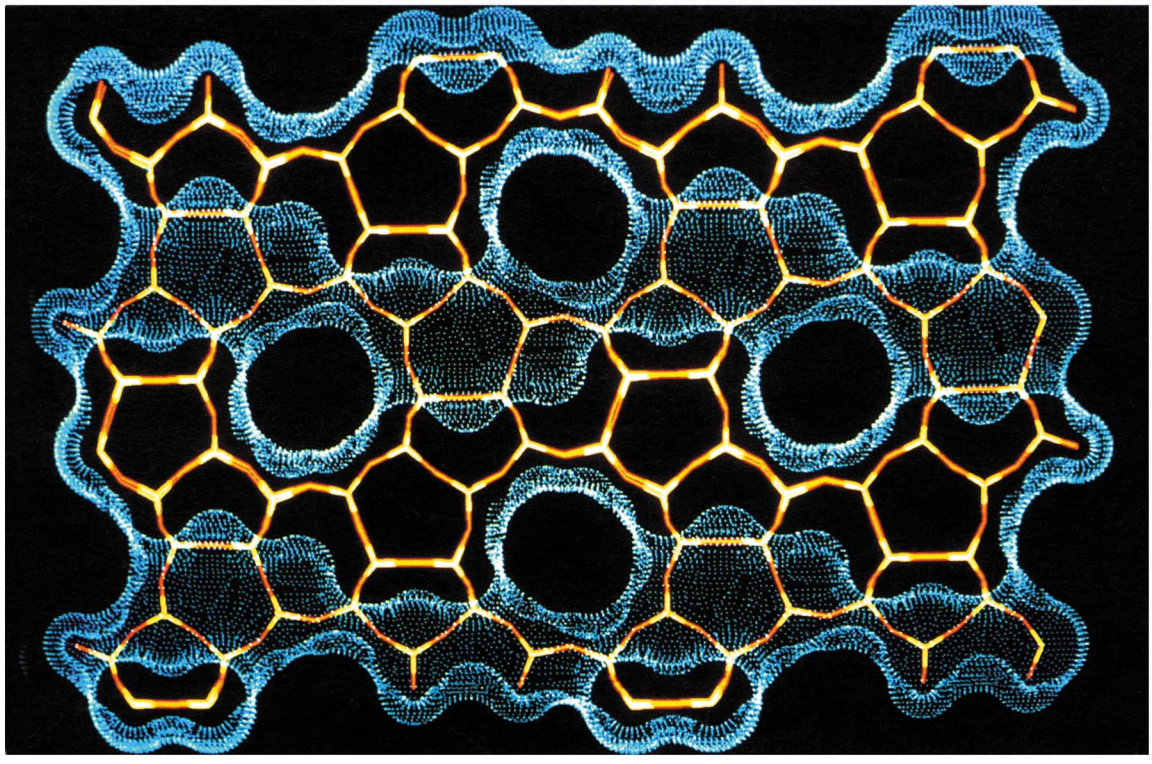

(*b*)

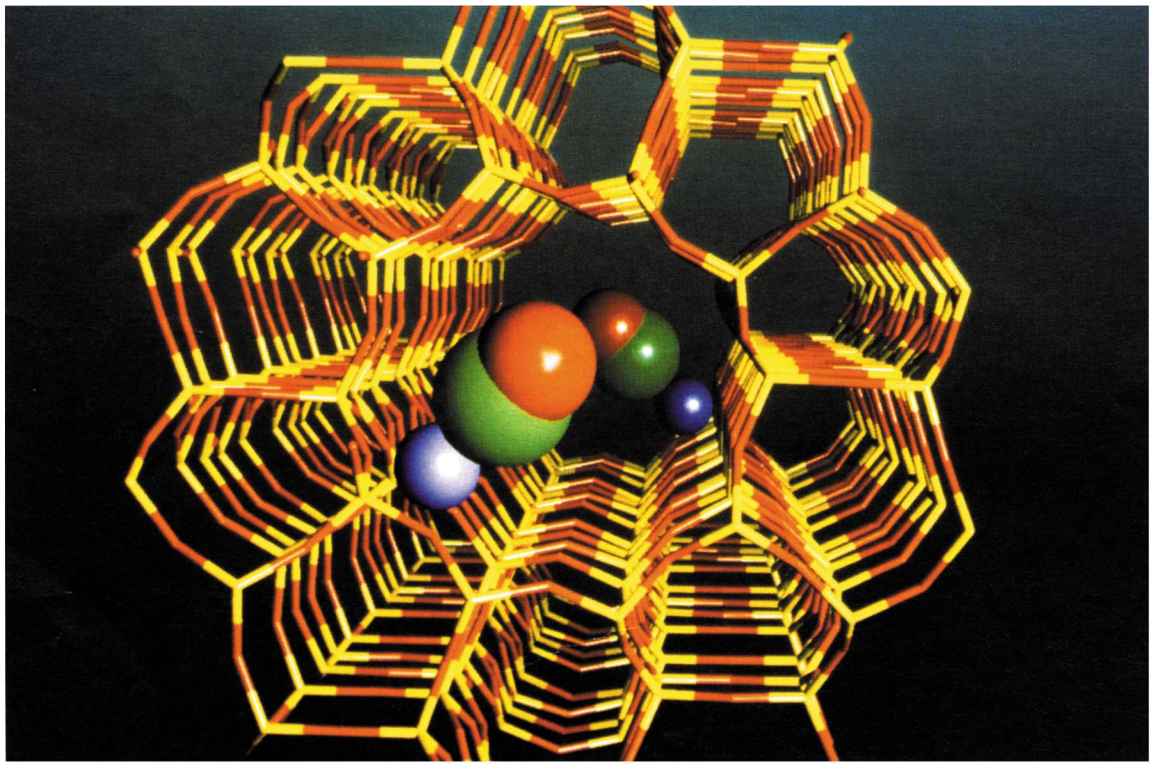

**Figure 5** (*a*) The structure of ZSM-5 viewed along the straight channels. The Connolly surface (defined by blue dots), obtained with a probe molecule 0.28 nm in diameter, clearly shows the second set of (sinusoidal) channels. (*b*) Enlarged view down a straight channel, showing extraframework cations ($Na^+$) with adsorbed CO molecules.

(band at 4075 $cm^{-1}$), but other less populated positions are also available, which are responsible for the shoulder at 4110 $cm^{-1}$. The important fact to be noted is that, when the low-frequency bands are considered, bathochromic shifts of the H−H stretching frequency (from the 4163 $cm^{-1}$ value of free $H_2$) increase with increasing ionicity of the zeolite framework (from Na-ZSM-5 to Na-A). However, for adsorbed CO the corresponding hypsochromic shifts were found to increase[17] in the opposite sense: highest for Na-ZSM-5 and lowest for Na-A. These results were rationalized in terms of the interaction modes discussed in Section 2.1. Dihydrogen is polarized by a cation and a neighbouring anion (Scheme 2), and the bathochromic shift of the H−H stretching frequency measures the

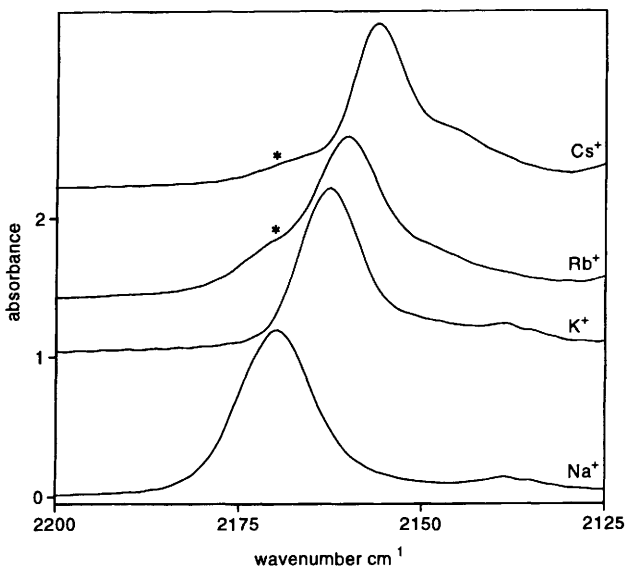


**Figure 6** IR spectra of CO adsorbed at 77 K on $M^+$ ZSM 5 (M = Na, K, Rb, Cs) The shift of the peak maximum from $Na^+$ to $Cs^+$ is clearly seen Note, however, that all spectra correspond to a CO equilibrium pressure of $10^2$ Pa For smaller CO doses all peaks shift to higher wavenumbers Corresponding values are given in the text The shoulder marked with an asterisk corresponds to a small fraction of $Na^+$ still present after ion exchange (Further details can be found in ref 27*a*)

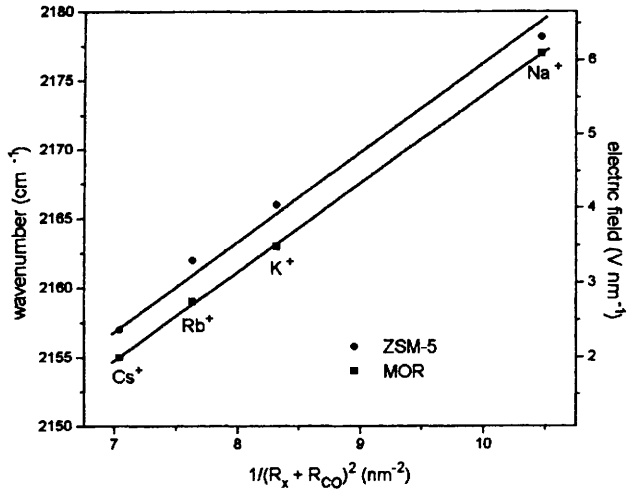


**Figure 7** C–O stretching frequency, and corresponding electric field, *versus* $1/(R_X + R_{CO})^2$ for alkali metal exchanged mordenites and ZSM 5 zeolites $R_X$ = cation radius

combined Lewis acid–base strength of the ion pair, while the electrostatic field sensed by the CO molecule is smaller when the negative contribution from framework anion is maximized, *i e* in the zeolite having highest ionicity Note that the local structure comprising a cation and a framework anion constitutes a dual acid–base site of the Lewis type, which plays an important role in many (catalytic) chemical processes mediated by zeolites Characterization of these dual sites is another example of the potential of IR spectroscopy using probe molecules

## 5 Extraframework Species and Lewis Acidity

During thermal dehydration, or steaming, the framework of zeolites (and zeotypes) tends to break up partially, and extraframework material is generated which remains entrapped in the zeolite channels The first stages of this process are represented in Scheme 5 Subsequent hydrolysis leads to detachment of $T(OH)_3$ or TOOH species (T = Al, Ga, Fe, *etc* ) with attendant formation of a silanol nest

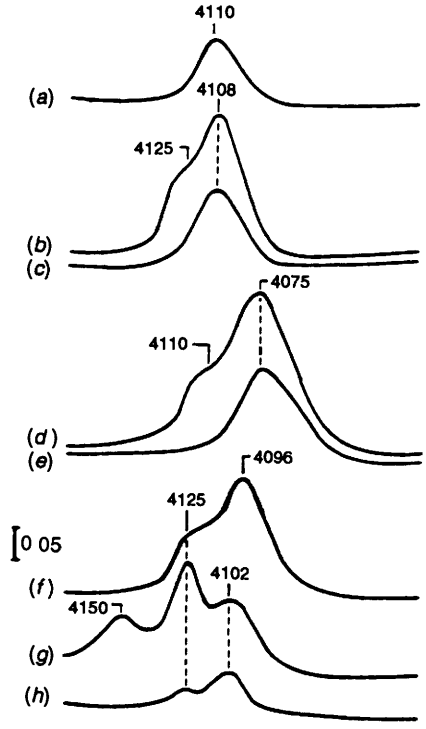


**Figure 8** Diffuse reflectance IR spectra of $H_2$ adsorbed at 77 K on (*a*) Na-ZSM 5, (*b*) and (*c*) Na MOR, (*d*) and (*e*), Na A, (*f*) Na X and (*g*) and (*h*) Na Y $P(H_2)$ = 0 3 kPa for (*a*), (*b*), (*e*), (*f*) and (*g*) or 13 kPa for (*c*) and (*d*) Spectrum (*h*) was taken after outgassing (77 K, 1 min) the Na Y zeolite sample with preadsorbed hydrogen
Reprinted with permission from ref 17

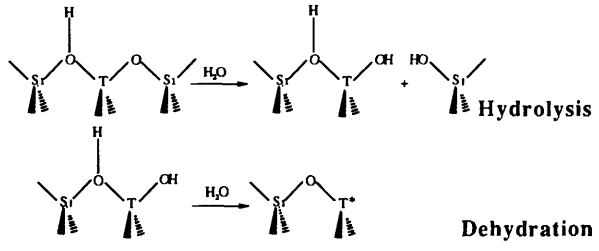


**Scheme 5**

The $T(OH)_3$ species thus formed can migrate and ultimately form, after clustering and dehydration, very small particles of a $T_2O_3$ phase Owing to steric constraints imposed by the zeolite framework, the dimensions of these clusters can be so small as to have a large proportion of coordinatively unsaturated T ions, which behave as strong Lewis acid centres

The high-frequency bands observed in Fig 4(*c*,*d*) correspond to CO and to $N_2$ coordinated to $Al^{3+}$ ions in extraframework species For CO a single band is observed, centred at 2225 cm $^{-1}$, while dinitrogen shows a more complex spectrum maximum at 2348 cm $^{-1}$ and shoulder around 2357 cm $^{-1}$ The 2348 cm $^{-1}$ band should correspond to $Al^{3+} \cdots N_2$ adducts in extraframework $Al_2O_3$, while the 2357 cm $^{-1}$ shoulder is tentatively assigned to the N–N stretching of $N_2$ interacting with highly exposed T* ions (partially extraframework) in Scheme 5 These species presumably exist only in a small concentration (because of ensuing hydrolysis), and carbon monoxide fails to detect them The enhanced specific absorbance of $N_2$ when subjected to high electric fields would explain its higher sensitivity (as compared to CO) for detecting strong Lewis acid centres

Fig 9(*a*) shows the relevant section of the IR spectra of CO adsorbed at 77 K on a sample of H-[Ga]ZSM-5 (Si/Ga = 25) previously activated at 823 K, so as to cause partial degalliation of the framework [32*a*] H-[Ga]ZSM-5 is analogous to H-ZSM-5, with gallium substituting for aluminium For comparison, the spectra of

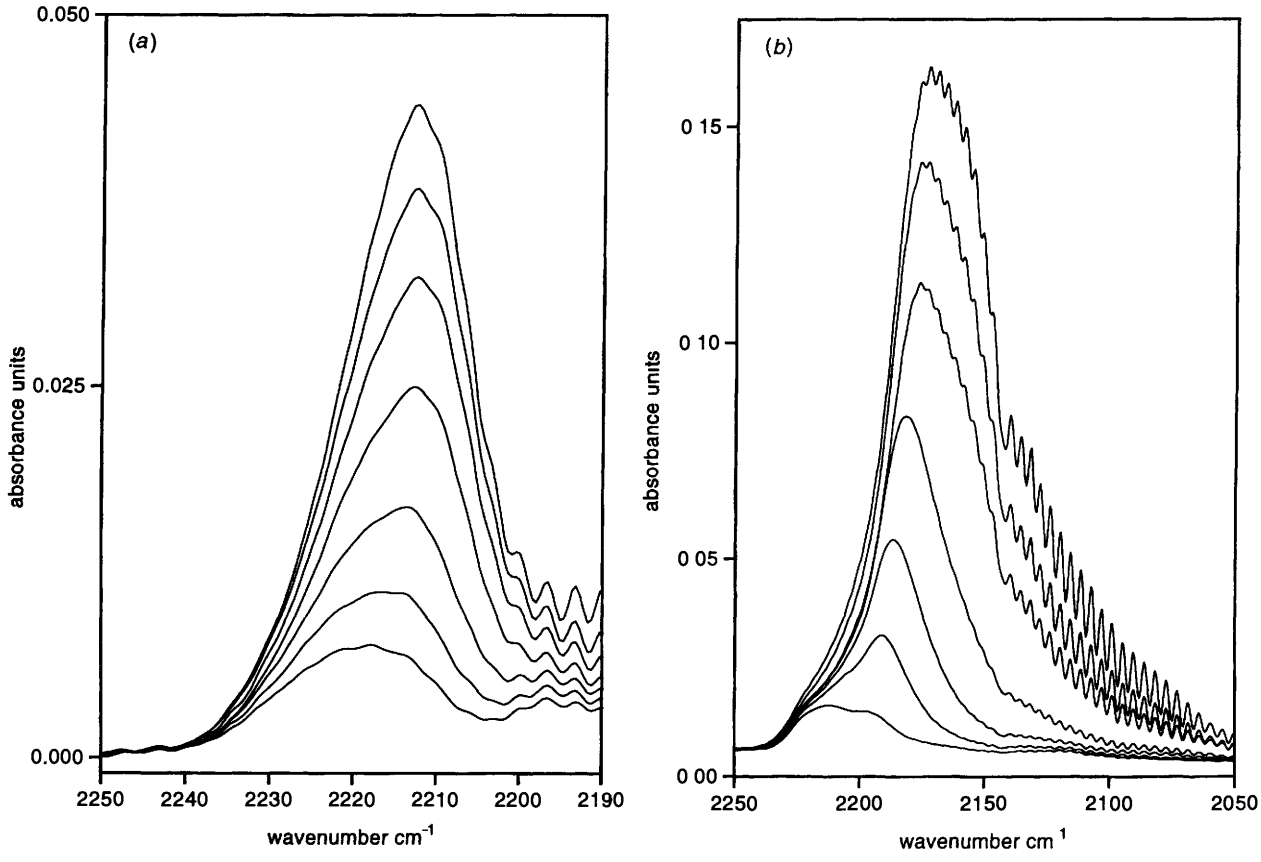


**Figure 9** (*a*) IR spectra of CO adsorbed at increasing equilibrium pressure (from $10^{-2}$ to 20 Torr) on extraframework '$Ga_2O_3$' species formed by partial degalliation of H-[Ga]ZSM 5, previously activated at 823 K *in vacuo* Spectra taken at liquid nitrogen temperature (*b*) CO adsorbed on finely divided gallium oxide, other details as in part (*a*)

CO adsorbed on finely divided $Ga_2O_3$ activated at the same temperature are also shown [Fig 9(*b*)] The main IR absorption band for $Ga_2O_3$ appears at 2190 cm $^{1}$, with a minor shoulder at 2220 $cm^{-1}$ The 2190 $cm^{-1}$ band corresponds to the C−O stretching of $Ga^{3+}$ ··· CO adducts formed on extended surfaces of the metal oxide, while the 2220 $cm^{-1}$ shoulder (which saturates at low CO equilibrium pressure) is assigned to similar adducts with more exposed $Ga^{3+}$ ions, *e g* in corners of $Ga_2O_3$ crystallites This assignment was made by comparison with IR spectra of CO adsorbed on $\gamma$-alumina [32b] It is noticeable that for the zeolite sample [Fig 9(*a*)] the 2220 $cm^{-1}$ band completely dominates the spectrum (the slight shift towards lower wavenumbers on increasing the CO doses is due to adsorbate–adsorbate interactions) thus proving the highly dispersed nature, and consequently high Lewis acidity, of the extraframework species, which do not seem to have undergone appreciable sintering The same conclusion (regarding extraframework aluminium species) was reported by Gruver and Fripiat,[23d] who studied Lewis acid sites in partially dealuminated mordenites As pointed out by these authors, the high dispersion degree of extraframework species should favour interaction with framework Brønsted acid sites, and consequent synergy in catalytic processes

## 6 Summary and Outlook

The use of diatomic molecular probes for rendering zeolites and zeotypes IR-readable has been outlined Information attainable using this technique concerns Brønsted and Lewis acidity, structural defects, internal electric fields and the siting of extraframework cations Specific examples were discussed which involve the most commonly used diatomic molecules CO, $N_2$ and $H_2$ Work with molecular oxygen was also recently reported [33] By choosing appropriate molecular probes, dual acid–base pairs can also be monitored, as shown for a series of Na-exchanged zeolites Detailed characterization of these dual sites should facilitate a better understanding of many (catalytic) chemical processes mediated by zeolites

Mid-IR spectroscopy of adsorbed molecules is a very active research field which contributes extensively to deepening our knowledge of the local structure of zeolite active sites, and of the physico-chemical properties of the intra-zeolite space This has strong bearing not only on heterogeneous catalysis and pollution control, but also on the potential use of zeolites as host materials for a variety of advanced composites which could find application in a number of technological fields, such as selective membranes, modified electrodes, chemical sensors or low-dimensional electrical conductors, to name only a few examples

Advances in zeolite characterization using IR molecular probes require detailed experimental research and precise knowledge about the spectroscopic response triggered by interaction of the probe molecule with the zeolite surface, this implies a close interplay between experimental work and theoretical studies The full power of quantum-chemical calculations and computer modelling techniques[13 33 34] is currently being applied (with very fruitful results) in conjunction with spectroscopic and structural research, and further developments are expected However, it should be acknowledged that elucidating all aspects of the structure and physico-chemical behaviour of zeolites is not an easy task, and concurrent use of several techniques is often required IR spectroscopy is but one of them, paramount among the others are X-ray and neutron diffraction,[19 35a] high resolution electron microscopy,[35d e] and MAS NMR spectroscopy [35e–i] Major contributions are also expected from techniques based on synchrotron radiation (XANES, EXAFS, PEXA, and time-resolved X-ray diffraction), particularly since they allow *in situ* studies of zeolite catalysts to be carried out under operating conditions [36] Altogether, the considerable efforts which are being made for an improved characterizaton of zeolites should result in a better understanding of their behaviour, and this should boost the many potential technological applications of these versatile materials

*Acknowledgements* We thank our collaborators, cited in specific references, who have contributed substantially to most of the experimental work discussed in this review The Spanish Ministerio de Educacion y Ciencia (DGICYT) is gratefully acknowledged for the award of the sabbatical stay of A Z at the Universidad de las Islas Baleares

## 7 References


1 M Estermann, L B McCusker, C Baerlocher, A Merrouche and H Kessler, *Nature*, 1991, **352**, 320
2 Q Huo R Xu, S Li, Z Ma, J M Thomas, R H Jones and A M Chippindale, *J Chem Soc Chem Commun*, 1992, 875
3 M E Davis, *Acc Chem Res*, 1993, **26**, 111
4 R Szostak, *Molecular Sieves*, Van Nostrand Reinhold, New York, 1989
5 G D Stucky, *Prog Inorg Chem*, 1992, **40**, 99
6 (*a*) G A Ozin, A Kuperman and A Stein, *Angew Chem Int Ed Engl*, 1989, **28**, 359, (*b*) G A Ozin, *Adv Mater*, 1992, **4**, 612
7 S Bordiga, G Ricchiardi, G Spoto, D Scarano, L Carnelli, A Zecchina and C Otero Arean, *J Chem Soc Faraday Trans*, 1993, **89**, 1843
8 M D Baker G A Ozin and J Godber, *Catal Rev Sci Eng*, 1985, **27**, 591
9 J W Ward, in *Zeolite Chemistry and Catalysis*, ed J A Rabo, ACS Monograph no 171, American Chemical Society, Washington, DC, 1976
10 N S Hush and M L Williams, *J Mol Spectrosc*, 1974, **50**, 349
11 G Pacchioni, G Cogliandro and P S Bagus, *Int J Quant Chem*, 1992, **42**, 1115
12 V Staemmler, *Chem Phys* 1975, **7**, 17
13 L Koubi, M Blain, E Cohen de Lara and J M Leclercq, *Chem Phys Lett*, 1994, **217**, 544
14 E Cohen de Lara and Y Delaval, *J Chem Soc Faraday Trans 2*, 1978, **74**, 790
15 W Kutzelnigg, V Staemmler and C Hoheisel, *Chem Phys*, 1973, **1**, 27
16 I N Senchenya and V B Kazansky, *Kinet Katal*, 1988, **29**, 1131
17 S Bordiga, E Garrone, C Lamberti, A Zecchina, C Otero Arean, V B Kazansky and L M Kustov, *J Chem Soc Faraday Trans*, 1994, **90**, 3367
18 A Zecchina, S Bordiga, G Spoto, L Marchese, G Petrini, G Leofanti and M Padovan, *J Phys Chem*, 1992, **96**, 4991
19 M Czjzek, H Jobic, A N Fitch and T Vogt, *J Phys Chem*, 1992, **96**, 1535
20 P A Jacobs and W J Mortier, *Zeolites*, 1982, **2**, 226
21 (*a*) S Bordiga, C Lamberti, F Geobaldo, A Zecchina, G Turnes Palomino and C Otero Arean, *Langmuir*, 1995, **11**, 527, (*b*) V L Zholobenko, M A Makarova and J Dwyer, *J Phys Chem*, 1993, **97**, 5962, (*c*) F Wakabayashi, J Kondo, K Domen and C Hirose, *J Phys Chem*, 1993, **97**, 10761
22 F Geobaldo, C Lamberti, G Ricchiardi, S Bordiga, A Zecchina, G Turnes Palomino and C Otero Arean, *J Phys Chem*, 1995, **99**, 11167
23 (*a*) H Knozinger, *Proc Int Symp Catal Sapporo*, 1988, ed K Tanabe *et al*, VCH, Weinheim, 1989, 146, (*b*) L Kubelkova, S Beran and J A Lercher *Zeolites*, 1989, **9**, 539, (*c*) M A Makarova, K M Al Ghefaili and J Dwyer *J Chem Soc Faraday Trans*, 1994, **90**, 383, (*d*) V Gruver and J J Fripiat, *J Phys Chem*, 1994, **98**, 8549, (*e*) K M Neyman, P Strodel, S P Ruzankin, N Schlensog, H Knozinger and N Rosch *Catal Lett* 1995, **31**, 273
24 E A Paukshtis and E N Yurchenko, *React Kinet Catal Lett*, 1981, **16**, 131
25 M A Makarova, A F Ojo, K Karim, M Hunger and J Dwyer, *J Phys Chem*, 1994, **98**, 3619
26 S Bordiga, E Escalona Platero, C Otero Arean, C Lamberti and A Zecchina, *J Catal*, 1992, **137**, 179
27 (*a*) A Zecchina, S Bordiga, C Lamberti, G Spoto, L Carnelli and C Otero Arean, *J Phys Chem*, 1994, **98**, 9577, (*b*) C Lamberti, S Bordiga, F Geobaldo, A Zecchina and C Otero Arean, *J Chem Phys*, 1995, **103**, 3158
28 (*a*) B Barrachin and E Cohen de Lara, *J Chem Soc Faraday Trans 2*, 1986, **82**, 1953, (*b*) H Bose and H Forster, *J Mol Struct*, 1990, **218**, 393
29 (*a*) G Spoto, A Zecchina, S Bordiga, G Ricchiardi, G Martra, G Leofanti and G Petrini, *Appl Catal*, 1994, **3B**, 150, (*b*) G Spoto, S Bordiga, G Ricchiardi, D Scarano, A Zecchina and F Geobaldo, *J Chem Soc Faraday Trans*, 1995, **91**, 3285, (*c*) Y Kuroda, Y Yoshikawa, S Konno, H Hamano, H Maeda, R Kumashiro and M Nagao, *J Phys Chem*, 1995, **99**, 10621
30 P Pelikan and R Boca, *Coord Chem Rev*, 1984, **55**, 55
31 L M Kustov and V B Kazansky, *J Chem Soc Faraday Trans*, 1991, **87**, 2675
32 (*a*) C Otero Arean, G Turnes Palomino, F Geobaldo and A Zecchina, *J Phys Chem*, 1996, **100**, 6678, (*b*) A Zecchina, E Escalona Platero and C Otero Arean, *J Catal*, 1987, **107**, 244
33 (*a*) F Jousse and E Cohen de Lara, *J Phys Chem*, 1996, **100**, 233, (*b*) F Jousse, A V Larin and E Cohen de Lara, *J Phys Chem*, 1996, **100**, 238
34 (*a*) G M Zhidomirov and V B Kazansky, *Adv Catal*, 1986, **34**, 131, (*b*) V B Kazansky, *Catal Today*, 1988, **3**, 367, (*c*) J Sauer, *Chem Rev*, 1989, **89**, 199, (*d*) L Kubelkova, S Beran and J A Lercher, *Zeolites*, 1989, **9**, 539, (*e*) *Modelling of Structure and Reactivity in Zeolites*, ed C R A Catlow, Academic Press, London, 1992, (*f*) J O Titiloye, S C Parker, F S Stone and C R A Catlow, *J Phys Chem*, 1991, **95**, 4038, (*g*) S J Cook, A K Chakraborty, A T Bell and D N Theodorou, *J Phys Chem*, 1993, **97**, 6679, (*h*) A G Pelmenschikov and R A van Santen, *J Phys Chem*, 1993, **97**, 10678, (*i*) G J Kramer, R A van Santen, C A Emeis and A K Nowak, *Nature*, 1993, **365**, 529, (*j*) J D Gale, C R A Catlow and J R Carruthers, *Chem Phys Lett*, 1993, **216**, 155, (*k*) D M Bishop, *Int Rev Phys Chem*, 1994, **13**, 21, (*l*) D M Bishop and S M Cybulski, *Chem Phys Lett*, 1994, **230**, 177, (*m*) R A van Santen and G J Kramer, *Chem Rev*, 1995, **95** 637, (*n*) A M Ferrari, P Ugliengo and E Garrone, *J Chem Phys*, submitted for publication
35 (*a*) L B McCusker, *Acta Crystallogr Sect A*, 1991, **A47**, 297, (*b*) G Vitale, L M Bull, B M Powell and A K Cheetham, *J Chem Soc Chem Commun*, 1995, 2253, (*c*) L M Bull, A K Cheetham, B M Powell, J A Ripmeester and C I Ratcliffe, *J Am Chem Soc*, 1995, **117**, 4328, (*d*) O Terasaki and T Ohsuna, *Catal Today*, 1995, **23**, 201, (*e*) J M Thomas, *Stud Surf Sci Catal*, 1989, **49A**, 3, (*f*) G Engelhardt and D Michel, *High Resolution Solid State NMR of Silicates and Zeolites*, Wiley, Chichester, 1987, (*g*) J Klinowski, *Annu Rev Mater Sci*, 1988, **18**, 189, (*h*) G Mirth, J Lercher, M W Anderson and J Klinowski, *J Chem Soc Faraday Trans*, 1990, **86**, 3039, (*i*) H Koller B Burger, A M Schneider, G Engelhardt and J Weitkamp, *Microporous Mater*, 1995, **5**, 219
36 J M Thomas and G N Greaves, *Science*, 1994, **265**, 1675